Preparation and Characterization of Glycoacrylate-Based Polymer-Tethered Lipid Bilayers on Benzophenone-Modified Substrates

Lisa Y. Hwang,[†] Heide Götz,[†,‡,§] Wolfgang Knoll,[||] Craig J. Hawker,[‡,⊥] and Curtis W. Frank*,[†]

Department of Chemical Engineering, Stanford University, Stanford, California 94305, IBM Almaden Research Center, 650 Harry Road, San Jose, California 95120, European Patent Office, Bayerstrasse 34, 80335 München, Germany, Max Planck Institute for Polymer Research, Ackermannweg 10, D-55128 Mainz, Germany, and Departments of Materials and of Chemistry and Biochemistry, University of California, Santa Barbara, California 93106

Received July 17, 2008. Revised Manuscript Received September 9, 2008

Polymer-tethered lipid bilayers are promising models for biological membranes as they may provide a soft, lubricating environment with sufficient spacing between the substrate and bilayer for incorporating transmembrane proteins. We present such a system that uses a glycoacrylate-based telechelic lipopolymer in combination with a lipid analogue. Characterization of the mixed monolayers of lipopolymers and free lipids at the air−water interface is used to examine the molecular organization that dictates the final assembly properties. Isotherms indicate that the source of the dominating interactions, whether polymer interactions in the subphase or alkyl chain interactions, depends on both the tethering density and area per molecule. Moreover, a critical composition exists at which the alkyl chain interactions dominate the monolayer behavior regardless of the area per molecule. Isobaric creep and hysteresis experiments suggest that permanent states due to irreversible polymer−polymer interactions are not created as the monolayer is compressed. These data, combined with theoretical polymer predictions, are used to understand the organization of the monolayers at the air−water interface and, hence, the separation distance between the bottom of the bilayer and substrate in the water-swollen state of the final bilayer assembly. Atomic force microscopy is used to confirm that the measured separation distance of 11.2 nm is on the order of what would be predicted using a theoretical analysis for a representative 5 mol % lipopolymer-tethered bilayer. Next, the homogeneity of the final bilayer is probed at multiple scales. Fluorescence microscopy is used to demonstrate that homogeneous and continuous bilayers can be formed (within the optical resolution limit of 500 nm) with all polymer tethering densities used in this study. Atomic force microscopy studies demonstrate that homogeneity comparable to that of a solid-supported lipid bilayer can be achieved for a representative 5 mol % lipopolymer-tethered bilayer. Langmuir−Blodgett transfer conditions for depositing monolayers that can be used to create homogeneous, fluid bilayers are also discussed. Finally, the distal leaflet lateral mobility is measured using fluorescence recovery after photobleaching experiments and shown to be a function of the tethering density. A possible model for the mobility data is developed in which the tethered lipids in the proximal leaflet act as immobile lipid obstacles that couple to distal leaflet lipids.

Introduction

Over 20 years ago, Brian and McConnell[1] first reported on the use of supported lipid bilayers, which have since become the most commonly used model membrane system. These bilayers assemble on a very thin lubricating layer of water that allows for lateral fluidity of the lipids[2−4] but is only a few nanometers in thickness.[5−7] Thus, the utility of this simple platform has been limited by the small separation distance between the bilayer and substrate, which is insufficient for housing proteins that have domains protruding from the membrane. While many variations building upon the solid-supported lipid bilayer have emerged,[8] one promising strategy designed to address this limitation incorporates a water-swollen, hydrophilic polymer that is tethered between the bilayer and substrate, which can increase the separation distance in a controlled fashion while maintaining a lubricating aqueous environment.[9] This polymer-tethered bilayer system is created using lipopolymers (polymers covalently linked to lipid analogues that integrate into the proximal leaflet of the bilayer) to stabilize the interface between the polymer and bilayer. Additional stability can be provided by covalent attachment of the polymer to the substrate. We have previously reported on a glycoacrylate-based polymer-tethered model membrane system that uses a random copolymer configuration, which would be targeted for applications requiring increased robustness and stability, but not requiring significant separation distances.[10] In this work, we utilize the same polymer chemistry, now in a telechelic lipopolymer configuration, to create a model membrane system that incorporates all of the advantages of a polymer tether

* To whom correspondence should be addressed. Phone: (650) 723-4573. Fax: (650) 723-9780. E-mail: curt.frank@stanford.edu.
[†] Stanford University.
[‡] IBM Almaden Research Center.
[§] European Patent Office.
[||] Max Planck Institute for Polymer Research.
[⊥] University of California.

(1) Brian, A. A.; McConnell, H. M. *Proc. Natl. Acad. Sci. U.S.A.* **1984**, *81*, 6159–6163.
(2) Tamm, L. K. *Biochemistry* **1988**, *27*, 1450–1457.
(3) Kalb, E.; Frey, S.; Tamm, L. K. *Biochim. Biophys. Acta* **1992**, *1103*, 307–316.
(4) Stelzle, M.; Miehlich, R.; Sackmann, E. *Biophys. J.* **1992**, *63*, 1346–1354.
(5) Bayerl, T. M.; Bloom, M. *Biophys. J.* **1990**, *58*, 357–362.
(6) Johnson, S. J.; Bayerl, T. M.; McDermott, D. C.; Adam, G. W.; Rennie, A. R.; Thomas, R. K.; Sackmann, E. *Biophys. J.* **1991**, *59*, 289–294.
(7) Koenig, B. W.; Krueger, S.; Orts, W. J.; Majkrzak, C. F.; Berk, N. F.; Silverton, J. V.; Gawrisch, K. *Langmuir* **1996**, *12*, 1343–1350.
(8) Sackmann, E. *Science* **1996**, *271*, 43–48.
(9) Spinke, J.; Yang, J.; Wolf, H.; Liley, M.; Ringsdorf, H.; Knoll, W. *Biophys. J.* **1992**, *63*, 1667–1671.
(10) Hwang, L. Y.; Götz, H.; Hawker, C. J.; Frank, C. W. *Colloids Surf., B* **2007**, *54*, 127–135.

10.1021/la8022997 CCC: $40.75
Published on Web 11/18/2008

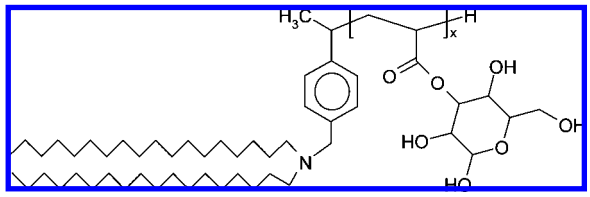

Figure 1. Structure of DODA-poly(D-glucose-2-propenoate) telechelic lipopolymer (GH24000).

such as a lubricating surface, an aqueous reservoir, and a means of covalent attachment to a wide variety of substrates while maintaining sufficient design flexibility in the final properties of the system including controlled separation distances and bilayer lateral fluidity.

We have designed our polymer-tethered lipid bilayer system and assembly process to meet several criteria that maximize its utility as a model membrane system. The polymer tether should provide a suitable environment for membrane components that may be incorporated into the bilayer. The telechelic lipopolymer used in this study is made up of D-glucose-2-propenoate repeat units and a terminal [4′-[(*N*,*N*-dioctadecylamino)methyl]phenyl]ethoxy (DODA) chain end. As discussed in our previous work,[10] the hydrophilic glycoacrylate-based backbone shares some characteristics of the native glycocalix, potentially improving the biocompatibility of this system. Next, the assembly process should facilitate straightforward control over the free lipid composition. For this study, we have chosen the commonly used L-α-phosphatidylcholine from egg (egg-PC) as the free lipid, which forms a liquid-phase monolayer over a large temperature range. The use of a film balance confers tremendous control over the organization of the molecules and conformation of the polymers, which is directly related to the separation distance. The next step involves a vertical Langmuir−Blodgett (LB) transfer of the organized monolayer onto a substrate that has been grafted with benzophenone moieties prior to the LB transfer. The transferred polymer is then covalently linked to the substrate through a photochemical reaction between substrate-bound benzophenone groups and adjacent C−H bonds in the polymer. Because this reaction is a rapid and efficient process that can occur in a variety of chemical environments,[11] it allows for significant flexibility in terms of both polymer chemistry and the substrate. Finally, the distal leaflet of the bilayer can be completed by fusing small unilamellar vesicles of egg-PC to the substrate-bound monolayer.

This study aims to systematically understand the organization and conformation of the assembly to predictably create well-defined polymer-tethered lipid bilayers that can be easily tailored according to the specific application design requirements.

Experimental Section

Lipopolymer. A glyco-based homopolymer made up of D-glucose-2-propenoate monomers and a terminal DODA group was synthesized by living free radical polymerization prior to this study.[12] This polymer has a polystyrene equivalent weight-average molecular weight (M_w) of 24 000 and a polydispersity of 1.16 (with THF as the carrier solvent).[13] The chemical structure of this telechelic lipopolymer (GH24000) is shown in Figure 1.

Substrate Preparation. Substrates for fluorescence experiments were glass coverslips, and substrates for AFM experiments were silicon wafers. (It should be noted that any substrate that can be functionalized with the benzophenone coupling agent could be used; silicon oxide substrates with surface silanol groups are being used as representative substrates.) Before use, the glass coverslips were immersed in ~85 °C 7× detergent (ICN Biomedicals, Inc.) at a 1:4 (v/v) dilution in Millipore water for at least 15 min, rinsed thoroughly in deionized (DI) water, dried under a N_2 stream, and baked in an oven for 4 h at 400 °C. Before use, the silicon wafer substrates were rinsed extensively in ethanol, dried under a N_2 stream, and cleaned in an oxygen plasma cleaner (March Plasmod plasma etcher from March Instruments, Inc.) at 75 W for 5 min.

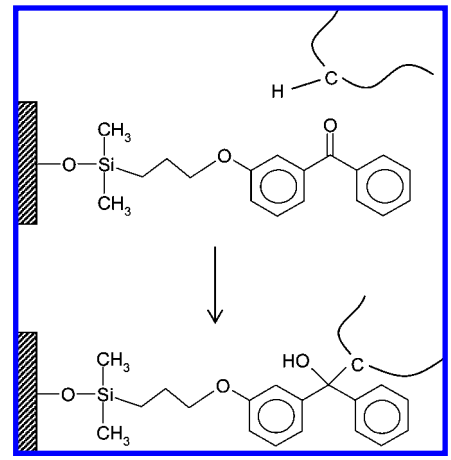

Figure 2. Covalent attachment of the lipopolymer to a benzophenone-modified substrate using UV illumination.

Immediately after being cleaned, the substrates were placed in an immobilization solution of 1.3 g/L 4-[[3′-(chlorodimethylsilyl)propyl]oxy]benzophenone in dry toluene. Synthesis of this benzophenone-based photocoupling group has been described previously.[14] Triethylamine, a catalyst and acid scavenger, was added at a ratio of 2:21 (v/v) triethylamine:immobilization solution. Substrates were kept in this solution under N_2 for 4−5 h at room temperature, followed by extensive substrate rinsing with toluene.

Film Balance Measurements and Langmuir−Blodgett Transfer. A 50 cm × 15 cm symmetric-compression Langmuir−Blodgett trough (KSV 5000) was used to perform all monolayer experiments at the air−water interface and LB transfers during which the Millipore water subphase temperature was maintained at 25.0 ± 0.2 °C. Stock solutions of GH24000 lipopolymer were made in 13:2 (v/v) chloroform:methanol due to the insolubility of GH24000 in pure chloroform. GH24000/egg-PC mixtures were prepared at various contents (mol %) of GH24000 with concentrations between 0.04 and 1.5 mg of lipid-like moiety/mL. The solvent was allowed to evaporate for 20 min before the barrier compression was started. The barrier compression rate was controlled at 5 mm/min forward speed and 2 mm/min backward speed. For LB transfers, a wait time of 30 min was used once the target surface pressure was reached prior to the transfer being started. During this wait time, the surface pressure was controlled and maintained by allowing the barriers to move. A transfer speed of 10.0 mm/min and a constant surface pressure of 25 mN/m were used for all LB transfers. This transfer speed was optimized as a function of the transfer pressure to determine the transfer conditions that produced homogeneous monolayers with transfer ratios approaching ideal.

Covalent Attachment to the Substrate. Directly following the LB transfer, the substrates with a transferred monolayer were exposed to UV light (λ > 340 nm) using a mercury UV lamp (Oriel Instruments) under ambient conditions for 5 min. This covalent attachment is illustrated in Figure 2.

Small Unilamellar Vesicles for Bilayer Formation. The standard extrusion method[15,16] was used to form small unilamellar vesicles (SUVs) composed of egg-PC (Avanti Polar Lipids), with or without

(11) Dorman, G.; Prestwich, G. D. *Biochemistry* **1994**, *33*, 5661–5673.
(12) Götz, H.; Harth, E.; Schiller, S. M.; Frank, C. W.; Knoll, W.; Hawker, C. J. *J. Polym. Sci., Part A: Polym. Chem.* **2002**, *40*, 3379–3391.
(13) Götz, H. Unpublished data.
(14) Prucker, O.; Naumann, C. A.; Rühe, J.; Knoll, W.; Frank, C. W. *J. Am. Chem. Soc.* **1999**, *121*, 8766–8770.

0.5 mol % *N*-(Texas Red sulfonyl)-1,2-dihexadecanoyl-*sn*-glycero-3-phosphoethanolamine, triethylammonium salt (Texas Red-PE; Molecular Probes), at a concentration of 5 mg/mL in Millipore water. A Mini-Extruder (Avanti Polar Lipids) was used to extrude the suspension through a 100 nm pore diameter polycarbonate membrane 31 times. The lipid vesicles were diluted with standard buffer (10 mM Tris, 100 mM NaCl adjusted to pH 8 using NaOH) to 2.5 mg/mL immediately prior to use. A droplet of this diluted solution sufficient to cover the entire substrate was placed in a clean Petri dish, and the substrate with an LB-transferred monolayer was gently placed facing downward on top of the droplet for 1 h to allow for complete vesicle fusion.

Atomic Force Microscopy. Atomic force microscopy (AFM) images were acquired on a MultiMode SPM with a Nanoscope IIIa controller (Digital Instruments). A Digital Instruments fluid cell was used for imaging in a liquid. Silicon nitride probes (Veeco model ORC8) were used for contact mode and tapping mode AFM. Typical scan rates of 0.4−2.5 Hz were used to record images on an E-type scanner, and a 512 pixels/line resolution was used for all images. Any vertical scanner drift, image bowing, skips, or other artifacts that may have resulted in offsets during scanning were minimized using flattening algorithms in the Nanoscope software. As imaging was done in a liquid (10 mM Tris, 100 mM NaCl adjusted to pH 8 using NaOH), several precautions were taken. The scanner was protected against liquid damage by covering the top with a thin film of Parafilm. Because fluid exchange was not needed, the rubber O-ring was not used in the fluid cell during imaging. However, the rubber O-ring was used during sample preparation prior to imaging to help keep the area of the sample within the O-ring under liquid at all times. The fluid cell and optical head were then mounted following standard liquid imaging procedures. After an equilibration time of approximately 1 h, imaging was commenced.

To measure the thickness of the tethered bilayer, small regions of the tethered bilayer were intentionally removed using contact mode AFM at a high scan rate (greater than 30 Hz) and a high force (∼30 nN) to measure the difference in vertical height. Once the bilayer regions were removed, the images were scanned using typical tapping mode AFM procedures.

Fluorescence Microscopy and Fluorescence Recovery after Photobleaching. The samples were imaged on a Nikon Eclipse E800 epifluorescent microscope using a 20× objective. Fluorescence emission was captured with a high-resolution Photometrics CoolSNAP HQ CCD camera (Roper Industries, Inc.). Images were processed with the Metamorph software package (Universal Imaging Corp.). To keep the bilayer protected and hydrated during imaging, another cleaned glass coverslip was placed on top of the bilayer while under water and then placed in a sample holder with two water reservoirs. Fluorescence recovery after photobleaching (FRAP) was used to determine the lateral diffusion coefficient. The Axelrod method, assuming a circular disk beam spot,[17] was used to analyze the data. The field diaphragm was contracted to ∼160 pixel diameter to create a circular photobleaching region. Following a 30 s photobleaching step, images of the fluorescence recovery were recorded. The fluorescence intensity of the photobleached region was measured as a function of time, with corrections for background counts and photobleaching due to image capture. A single-exponential decay was used to fit the data, and this recovery curve was used to determine the fluorophore lateral diffusion constant, D:

$$D = 0.22\frac{w^2}{\tau_{1/2}} \quad (1)$$

In eq 1, $\tau_{1/2}$ is the time at which the intensity has recovered to half of $F(\infty)$, the intensity at infinite time (from the data fit), and w is the diameter of the photobleaching region.

Results

Monolayer Properties at the Air−Water Interface. Surface pressure−area isotherms of GH24000/egg-PC mixed monolayers at different molar concentrations of 0, 0.5, 3, 5, 10, 20, and 100 mol % GH24000 are shown in Figure 3. Below ∼30 mN/m, an expansion of the monolayer to larger average molecular areas is seen in all mixtures as the percentage of GH24000 in the monolayer is increased. The typical isothermal behavior indicative of polymer pancake−mushroom−brush conformational transitions in the subphase[18] is seen for all mixtures containing 3 mol % GH24000 or higher. The slight expansion of the 0.5 mol % GH24000 isotherm at lower surface pressures indicates that there may be some subtle interactions of the polymer in the subphase, but the isotherm has essentially the same shape as the 0 mol % GH24000 (pure egg-PC) isotherm. Significantly, it does not show the transition typically associated with desorption of the polymer from the interface into the subphase. At high surface pressures above 30 mN/m, little difference is observed in the isotherms for 0−10 mol % GH24000. This indicates that the hard-core repulsion of the alkyl chains is dominant relative to the interactions of the polymer in the subphase at these high surface pressures. However, the 20 and 100 mol % GH24000 isotherms are shifted to larger molecular areas even at high surface pressures. It is likely that at these higher tethering densities the energy required to stretch the polymer chains even further normal to the interface is large enough to prohibit the monolayers from reaching the smaller molecular areas at which alkyl chain interactions similar to the lower GH24000 tethering densities are observed.

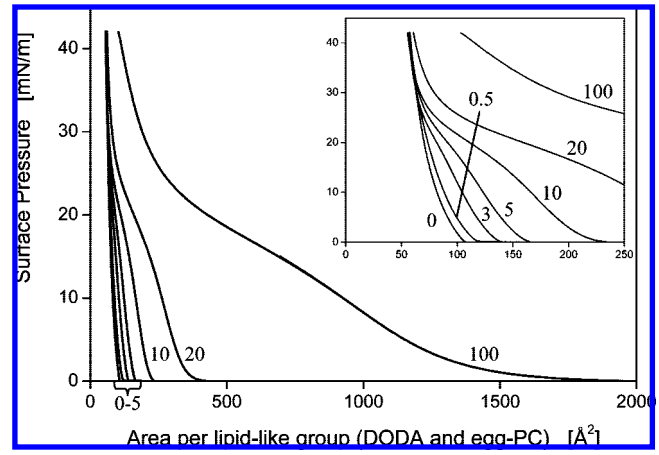

Figure 3. Langmuir isotherms of GH24000/egg-PC mixed monolayers at 25.0 °C. The isotherms were recorded for 0, 0.5, 3, 5, 10, 20, and 100 mol % GH24000. The inset shows an enlarged view of the isotherms at smaller average areas per lipid-like group.

This expansion of average molecular area measured at higher surface pressures can be quantified using the "limiting area" of the monolayer. The high-pressure, linear portion of the isotherm can be extrapolated back to the x-axis where $\pi = 0$ mN/m to obtain the limiting area, which describes the average area per molecule in a hypothetical state of uncompressed close-packed configuration. Table 1 shows the limiting areas for the mixed monolayers, as well as the limiting area of DODA obtained from the literature. Note that this value for the limiting area of DODA was determined at 28 °C. At 25 °C, the limiting area will likely be slightly smaller than 23.1 Å^2. Although the limiting areas for 0−10 mol % GH24000 monolayers are essentially identical, the

(15) Mayer, L. D.; Hope, M. J.; Cullis, P. R. *Biochim. Biophys. Acta* **1986**, *858*, 161–168.
(16) MacDonald, R. C.; MacDonald, R. I.; Menco, B. P. M.; Takeshita, K.; Subbarao, N. K.; Hu, L. R. *Biochim. Biophys. Acta* **1991**, *1061*, 297–303.
(17) Axelrod, D.; Koppel, D. E.; Schlessinger, J.; Elson, E.; Webb, W. W. *Biophys. J.* **1976**, *16*, 1055–1069.
(18) Baekmark, T. R.; Elender, G.; Lasic, D. D.; Sackmann, E. *Langmuir* **1995**, *11*, 3975–3987.

Table 1. Limiting Areas of GH24000/Egg-PC Mixed Monolayers at 25.0 °C

	limiting area (Å^2/molecule)
0% GH24000	79
0.5% GH24000	80
3% GH24000	78
5% GH24000	79
10% GH24000	80
20% GH24000	99
100% GH24000	345
DODA	23.1[a]

[a] For DODA at 28 °C.[19]

limiting areas for 20 and 100 mol % GH24000 shift to larger areas. This cannot simply be due to the change in the lipid-like component composition since the limiting area of DODA is actually smaller than that of egg-PC. It is clear that the polymer interactions in the subphase are driving the increase in limiting area with increasing percentage of GH24000.

As with any multicomponent monolayer, a concern for these tethered lipid bilayer systems is that segregation between the lipopolymers and free lipids, due to either polymer−polymer interactions in the subphase or mismatch between the lipid tethered to the polymer (DODA) and the free lipid (egg-PC), may lead to the formation of macroscopic domains in the proximal lipid leaflet. Therefore, hysteresis experiments were performed to investigate the reversibility of molecular interactions occurring within the monolayer during compression. As discussed above, all mixed monolayers containing 3 mol % GH24000 or more exhibited transitions reflective of polymer conformational changes in the subphase. The 5 mol % GH24000 was chosen for hysteresis experiments as a representative mixed monolayer for investigating the reversibility of the polymer interactions.

Figure 4 shows two compression and expansion cycles for 5 mol % GH24000 with an upper surface pressure limit of 18.6 mN/m (Figure 4a) or 25.0 mN/m (Figure 4b) with no delay between each step. The surface pressure of 18.6 mN/m was chosen because it is in the regime in which the polymer exists in the mushroom conformation; at 25.0 mN/m, the polymer is extended normal to the interface. Figure 4a shows that the isothermal behavior of the monolayer when cycling between an expanded pancake conformation and mushroom conformation (i.e., just prior to the point where polymer−polymer interactions drive the polymer to extend normal to the interface) is essentially reversible. Figure 4b shows a shift toward smaller average molecular areas after the first compression cycle. However, the general shape of the isotherm is unchanged, and the polymer in the subphase appears to sample the same polymer conformations for all subsequent steps. Thus, it is unlikely that any irreversible polymer−polymer interactions that would prohibit the polymers from returning to the mushroom or pancake conformations (for example, water-mediated network formation[20]) are present. The source of the shift to smaller molecular areas observed after the first compression may simply be due to a lack of relaxation time permitted after each cycle since each cycle was run with no delay before the following cycle was started.

The hysteresis results presented in Figure 4 do not probe cohesive lipid interactions as they were conducted below 30 mN/m (surface pressure at which the alkyl chain interactions dominate the film behavior). However, our previous studies on the random copolymer based on the same lipopolymer chemistry[10] showed that permanent condensed states were not formed at surface pressures up to 35 mN/m, although the possibility of phase separation within the monolayer cannot be eliminated. Thus, it is reasonable to conclude that permanent condensed states are also not formed in these GH24000/egg-PC mixed monolayers.

Isobaric creep experiments were performed on the mixed monolayers to study the stability at the air−water interface. Figure 5 shows the average area per lipid-like group (or "mean molecular area", MMA), normalized by the MMA at time zero when the monolayer first reaches the target surface pressure, with the holding time for the mixed monolayers held at a constant pressure of 25 mN/m. The creep increases with increasing percentage of GH24000 in the monolayer.

Isobaric creep experiments were also performed at additional surface pressures. Figure 6 summarizes the isobaric creep results for surface pressures of 10, 25, 30, and 32 mN/m. The normalized MMA after 30 min of holding at each surface pressure is plotted as a function of the molar percentage of GH24000. At a holding pressure of 10 mN/m, the creep after 30 min appears to be relatively constant (2% decrease in MMA) regardless of the monolayer composition. As this surface pressure is below the threshold at which polymers begin to interact significantly, the main difference between these monolayers is the DODA: egg-PC ratio. Thus, we can conclude that the effects of DODA and egg-PC on monolayer stability appear to be indistinguishable at this low surface pressure. We can also isolate the effect of the surface pressure on the creep of pure lipids (0 mol % GH24000). The stability of the pure egg-PC monolayer decreases as the holding pressure is increased. Although the alkyl chains of the monolayer are in a state of higher organization at higher surface pressures, the high surface pressures may cause buckling or loss of material. The effect is relatively small as the average molecular area decreases from 2% at 10 mN/m to only 9% at 32 mN/m.

The amount of polymer in the monolayer, however, clearly has a much larger effect on the monolayer stability. As the percentage of GH24000 in the monolayer is increased, the decrease in stability becomes more and more substantial. For 100 mol % GH24000, the average molecular area decreases from 2% at 10 mN/m to 36% at 32 mN/m. At this high surface pressure, the energy required for the polymer to remain stretched in an extended brush conformation may be too great, resulting in a loss of material or even buckling of the monolayer in the third dimension perpendicular to the air−water interface.[21] This increased creep beyond what is seen with the pure lipid film could also be a result of equilibration and relaxation of the polymer in the subphase (without loss of material or buckling). However, it does not appear that an extended brush conformation is unstable, in general. The decrease in average molecular area for 100 mol % GH24000 at 25 mN/m (also in an extended brush conformation) is only half of that at 32 mN/m. In addition, the creep observed for 5 mol % GH24000 at 25 mN/m, which is in a brush conformation, is approximately the same as the 0 mol % GH24000 monolayer creep observed at 32 mN/m.

The creep data can also be used to aid in the choice of transfer pressure for creating our model membranes. Because the overall intent of these monolayers is to create bilayers that are suitable environments for housing transmembrane proteins, the lipid packing and organization should be similar to that of biological membranes. We would also like to create membranes that are as stable and robust as possible. The average area per molecule

(19) Shen, W. W. Ph.D. Dissertation, Stanford University, Stanford, CA, 2002.

(20) Naumann, C. A.; Brooks, C. F.; Wiyatno, W.; Knoll, W.; Fuller, G. G.; Frank, C. W. *Macromolecules* **2001**, *34*, 3024–3032.

(21) Majewski, J.; Kuhl, T. L.; Gerstenberg, M. C.; Israelachvili, J. N.; Smith, G. S. *J. Phys. Chem. B* **1997**, *101*, 3122–3129.

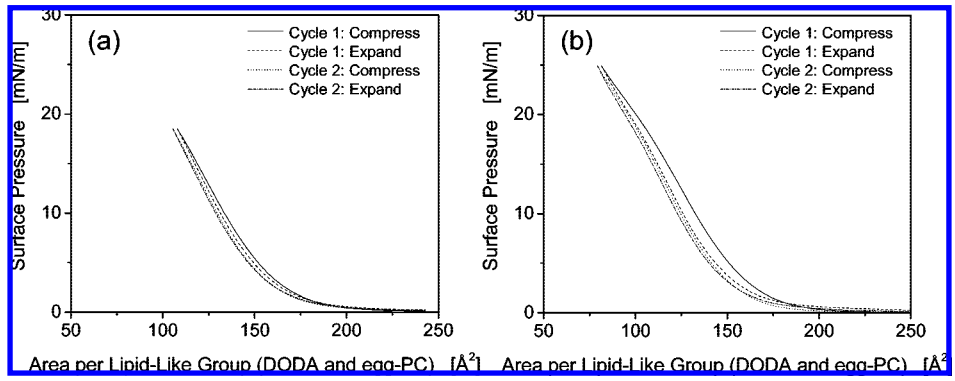

Figure 4. Compression and expansion cycles of 5 mol % GH24000 up to (a) 18.6 mN/m or (b) 25.0 mN/m.

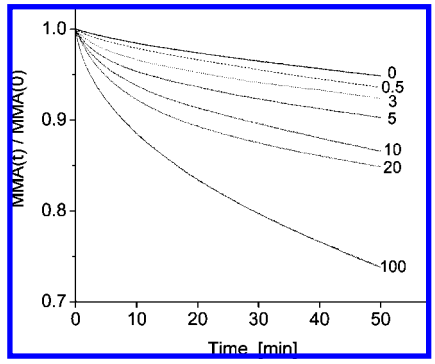

Figure 5. Isobaric creep experiments at a surface pressure of 25 mN/m for increasing mole fractions of GH24000 in mixed monolayers of GH24000 and egg-PC: 0, 0.5, 3, 5, 10, 20, and 100 mol % GH24000 at $T = 25.0$ °C.

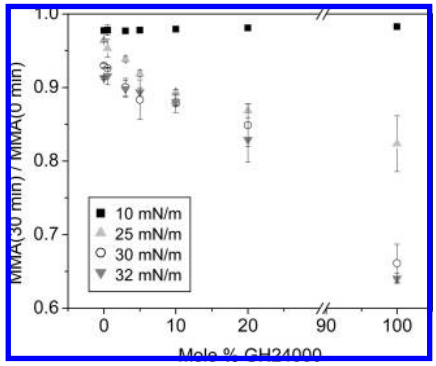

Figure 6. Summary of isobaric creep after 30 min at $T = 25.0$ °C for mixed monolayers of GH24000 and egg-PC at 0, 0.5, 3, 5, 10, 20, and 100 mol % GH24000. The isobaric creep was recorded at four different surface pressures of 10, 25, 30, and 32 mN/m.

in an egg-PC bilayer has been reported to be 64 Å^2.[22] From the 0 mol % GH24000 (pure egg-PC) isotherm that is shown in Figure 3, this corresponds to ~29 mN/m surface pressure in the monolayer. However, the isobaric creep studies show that significant creep is observed in the mixed monolayers at 30 mN/m (corresponding average molecular area for pure egg-PC, 63 Å^2) and 32 mN/m (corresponding average molecular area for pure egg-PC, 62 Å^2), whereas only moderate creep is observed at 25 mN/m (corresponding average molecular area for pure egg-PC, 66 Å^2). Therefore, a transfer pressure of 25 mN/m, which has a corresponding average molecular area of egg-PC that is within 3% of that reported for the bilayer, was chosen to create stable mixed monolayers for further studies. The additional space in the monolayer at 25 mN/m may also provide an environment that is more receptive to incorporating proteins that integrate into the membrane.

Bilayers. Mixed GH24000/egg-PC monolayers were transferred onto substrates using LB transfer, and the distal leaflets of the bilayers were completed using vesicle fusion. Figure 7 shows fluorescence images of bilayers formed on 0, 0.5, 3, 5, 10, 20, and 100 mol % GH24000 monolayers, as well as a solid-supported lipid bilayer (SSLB) control. For the mixed monolayers, egg-PC vesicles labeled with 0.5 mol % Texas Red-PE were used to complete the distal leaflets of the bilayers. The SSLB control was formed by vesicle fusion of the 0.5 mol % Texas Red-PE vesicles directly onto a clean glass coverslip. The images show that homogeneous bilayers, at the resolution limit of the fluorescence microscope, can be formed on all of these mixed monolayers prepared using LB transfer. For the 20× objective used for all of the images in Figure 7, the lateral resolution is 500 nm.

To investigate the lateral fluidity of the polymer-tethered lipid bilayers, we used FRAP experiments to determine lateral diffusion coefficients and mobile fractions. In these experiments, the distal leaflets of the bilayers were completed by fusing vesicles labeled with 0.5 mol % Texas Red-PE to the LB-transferred monolayers. It has been reported that little to no interleaflet lipid mixing occurs during vesicle fusion to a monolayer.[3] Thus, we assume that the lipid probes remain in the distal leaflet and probe the distal leaflet fluidity. A summary of the diffusion data for all GH24000 mixtures is shown in Figure 8. Also shown are values for an SSLB control on glass ($D = 5.1 \pm 1.5$ μm^2/s, mobile fraction 86 ± 6%). This is well within the range of diffusion coefficients that have been reported for bilayers on glass (1−8 μm^2/s)[1,4,23] and provides a quantitative basis for comparison of the diffusion coefficients measured for the GH24000-tethered lipid bilayers. The diffusion coefficients for the 0 and 0.5 mol % GH24000 bilayers are comparable to that of the SSLB control, but the diffusion coefficients for the 3−20 mol % GH24000 bilayers rapidly decrease with increasing percentage of GH24000. No recovery was observed in the 100 mol % GH24000 bilayer during FRAP experiments. The mobile fractions of the bilayers shown in Figure 8b also appear to decrease with increasing percentage of GH24000, though in a linear fashion. This is similar to what has been reported previously for other polymer-tethered bilayer systems using *distal* leaflet lipid probes.[24,25] However, several reports on *proximal* leaflet lipid probe mobility show

(22) McIntosh, T. J.; Magid, A. D.; Simon, S. A. *Biochemistry* **1989**, *28*, 7904–7912.

(23) Tamm, L. K.; McConnell, H. M. *Biophys. J.* **1985**, *47*, 105–113.
(24) Wagner, M. L.; Tamm, L. K. *Biophys. J.* **2000**, *79*, 1400–1414.
(25) Naumann, C. A.; Prucker, O.; Lehmann, T.; Ruhe, J.; Knoll, W.; Frank, C. W. *Biomacromolecules* **2002**, *3*, 27–35.

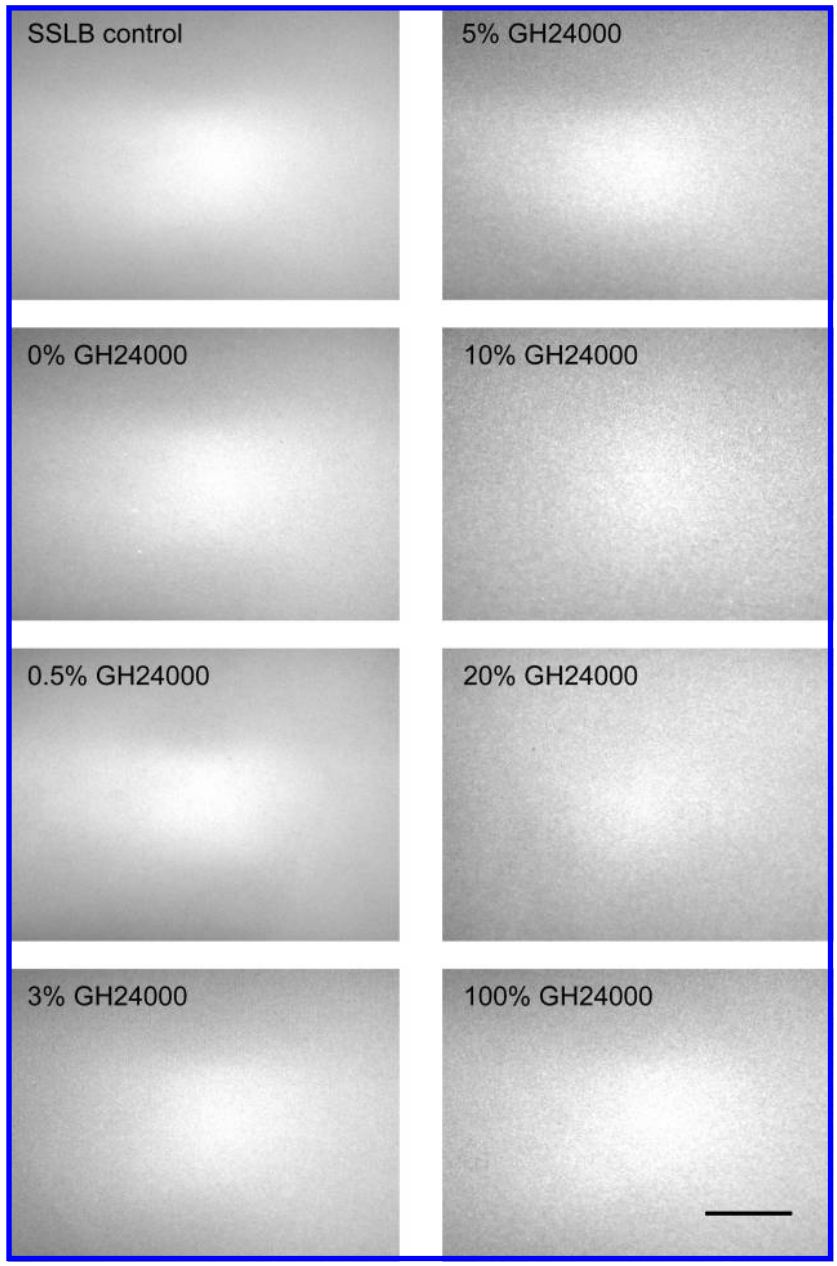

Figure 7. Fluorescence images of bilayers formed on mixed monolayers of GH24000 and egg-PC. Vesicle fusion with egg-PC vesicles labeled with 0.5 mol % Texas Red-PE was used to complete the distal leaflets of the bilayers. As a control, the labeled vesicles were also used to form an SSLB directly on glass, which is shown in the first image. All of the images were taken using a 20× objective. The scale bar indicated in the final image represents 100 μm.

that the diffusion coefficient decreases linearly with increasing percentage of lipopolymer and that the mobile fraction remains constant until a critical percentage of tethering is reached, at which point a drastic reduction is observed.[26,27]

Although fluorescence microscopy is very useful for investigating long-range lateral mobility and homogeneity of the bilayers, the lateral resolution is typically on the order of several hundreds of nanometers (500 nm for the experimental setup used in these studies). By contrast, AFM can reach lateral resolutions on the order of 2−10 nm. In addition, this technique does not require the incorporation of a probe molecule and was used to further investigate the homogeneity of the tethered bilayers. Figure 9 shows a tapping mode AFM image of a 5 mol % GH24000 bilayer imaged in standard buffer. Vesicle fusion with unlabeled egg-PC vesicles was used to complete the distal leaflet of this bilayer. For comparison, an SSLB formed by vesicle fusion directly onto the substrate was also imaged under the same conditions. This figure demonstrates that a comparable homogeneity is achieved in the GH24000-tethered bilayer relative to the solid-supported lipid bilayer. Both samples show a relatively low mean roughness, R_a, of less than 0.2 nm. This is well below values reported for other polymer-tethered lipid bilayers (rms = 2.9 nm)[28] and is on the order of values reported for lipid bilayers on glass (rms < 0.3 nm).[29] A few small holes

(26) Deverall, M. A.; Gindl, E.; Sinner, E. K.; Besir, H.; Ruehe, J.; Saxton, M. J.; Naumann, C. A. *Biophys. J.* **2005**, *88*, 1875–1886.
(27) Purrucker, O.; Fortig, A.; Jordan, R.; Tanaka, M. *ChemPhysChem* **2004**, *5*, 327–335.
(28) Shao, Y.; Jin, Y. D.; Wang, J. L.; Wang, L.; Zhao, F.; Dong, S. J. *Biosens. Bioelectron.* **2005**, *20*, 1373–1379.
(29) Schönherr, H.; Johnson, J. M.; Lenz, P.; Frank, C. W.; Boxer, S. G. *Langmuir* **2004**, *20*, 11600–11606.

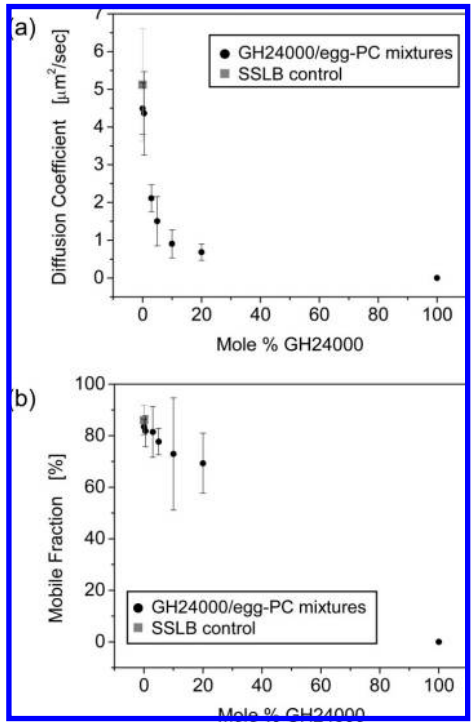

Figure 8. Lateral mobility data from FRAP measurements. Vesicle fusion with vesicles containing 0.5 mol % Texas Red-PE was used to label the distal leaflets of the bilayers. Lateral diffusion coefficients (a) and mobile fractions (b) of Texas Red-PE in GH24000-tethered lipid bilayers are shown as a function of the content (mol %) of GH24000. As a control, the Texas Red-PE labeled vesicles were also used to form SSLBs directly on glass. The corresponding measurements for the SSLB control are shown as indicated in each graph. Each data point represents the average of at least six measurements from 3−4 different samples.

or depressions, typical of defects seen in these bilayers, can be seen in the 10 × 10 μm images. The defects shown in the 5 mol % GH24000-tethered bilayer image range from 200 to 300 nm in the widest dimension, and the vertical distance of these defects is ∼2.2 nm. The defects in the SSLB control range from 100 to 200 nm in the widest dimension, and the vertical distance of these defects is ∼2.3 nm.

In addition to providing a means to examine the homogeneity of the bilayer at high lateral resolution, AFM provides a means to measure the thickness of the overall polymer-tethered lipid bilayer assembly with high vertical resolution on the order of angstroms. The thickness of a 5 mol % GH24000-tethered bilayer was studied by removing a small region of the tethered bilayer with high-force contact mode AFM at high scan rates. Then, the same area on the bilayer was imaged using the tapping mode to determine a vertical distance of 16.2 nm, as shown in Figure 10. The measured vertical distance includes the thickness of the egg-PC bilayer, which is 5.0 nm.[22,29] Thus, the separation distance between the substrate and bilayer for the 5 mol % GH24000-tethered bilayer is determined to be 11.2 nm.

Discussion

Separation Distance. Our goal is to develop well-defined, tailorable polymer-tethered bilayers with separation distances between the bilayer and substrate that may be suitable for incorporating a wide variety of transmembrane proteins. Therefore, understanding the conformational behavior of the lipopolymers used to create the cushion between the bilayer and surface is critical to predicting and controlling this separation distance. The conformational behavior can depend on many factors including the chemistry, molecular weight, and tethering density of the polymer. Flory theory of a polymer in a good solvent can be used to model the swollen polymers when the average distance between graft sites, s, is large enough that the polymers do not interact with each other:

$$R_F = aN^{3/5} \tag{2}$$

In eq 2, a is the Kuhn segment length and N is the number of Kuhn segments. Thus, for tethering densities in which $s \geq R_F$, the upper limit for the extension length of the polymer into the subphase, L, is R_F. When the tethering density of the polymer is high enough such that $s < R_F$, the polymers will extend further into the subphase, forming a brush conformation that can be predicted using the de Gennes theory for polymers anchored to an interface and in a good solvent:[30]

$$L = \frac{Na^{5/3}}{s^{2/3}} \tag{3}$$

The average distance between graft sites, s, is given by the following equation, where A is the area of a lipid molecule and f is the mole fraction of lipopolymer in the monolayer:

$$s = \left(\frac{A}{f}\right)^{1/2} \tag{4}$$

The chemistry of the lipopolymer can dramatically affect the conformation and must be taken into account by using an equivalent freely jointed chain of Kuhn segments when the theories are applied to a real polymer system. The Kuhn segment length of our lipopolymer is not known, but can be estimated from those of other polymers. Similar to polystyrene, our glycoacrylate lipopolymer has a C−C backbone and large, bulky side groups. Thus, we will use the equivalent freely jointed chain parameters for polystyrene to estimate values for our lipopolymer (see Table 2). Using these values, the predicted polymer conformation behavior at a surface pressure of 25 mN/m (A = 66 Å^2 for egg-PC on the basis of Figure 3) is shown in Figure 11. The mushroom-to-brush transition is predicted to occur starting at 0.8 mol % GH24000. This agrees well with the isothermal behavior seen in the isotherms (Figure 3) as discussed.

It is important to emphasize the necessity of using appropriate Kuhn segment values when polymer theories that are based on freely jointed models are applied to real polymeric systems. Incorrect calculations in which the number of monomer units and monomer lengths are used instead of the number of Kuhn segments and Kuhn lengths can lead to significant error in predicting polymer behavior. For example, if monomer values for the GH24000 lipopolymer were used to theoretically treat the polymer behavior, the mushroom-to-brush transition would be predicted to occur at 4 mol % GH24000 (R_F = 41 Å). This is confirmed to be erroneous as polymer transitions in the subphase are clearly observed in the 3 mol % GH24000 isotherm in Figure 3. Improper usage of monomer values instead of Kuhn segment values in recent literature on lipopolymer behavior has led to reported discrepancies between the theory and measured data for several lipopolymer systems. For instance, Wagner and Tamm[24] reported on a poly(ethylene glycol) (PEG) based lipopolymer. Using the de Gennes theory, they calculated that the mushroom-to-brush transition should occur at 3.1 mol % lipopolymer on the basis of monomeric values of 77 repeat units and a monomeric length of 3.5 Å. However, evidence of mushroom-to-brush transitional behavior was seen in the monolayer isotherms down to 1.0 mol % lipopolymer. Using

(30) de Gennes, P. G. *Adv. Colloid Interface Sci.* **1987**, *27*, 189–209.

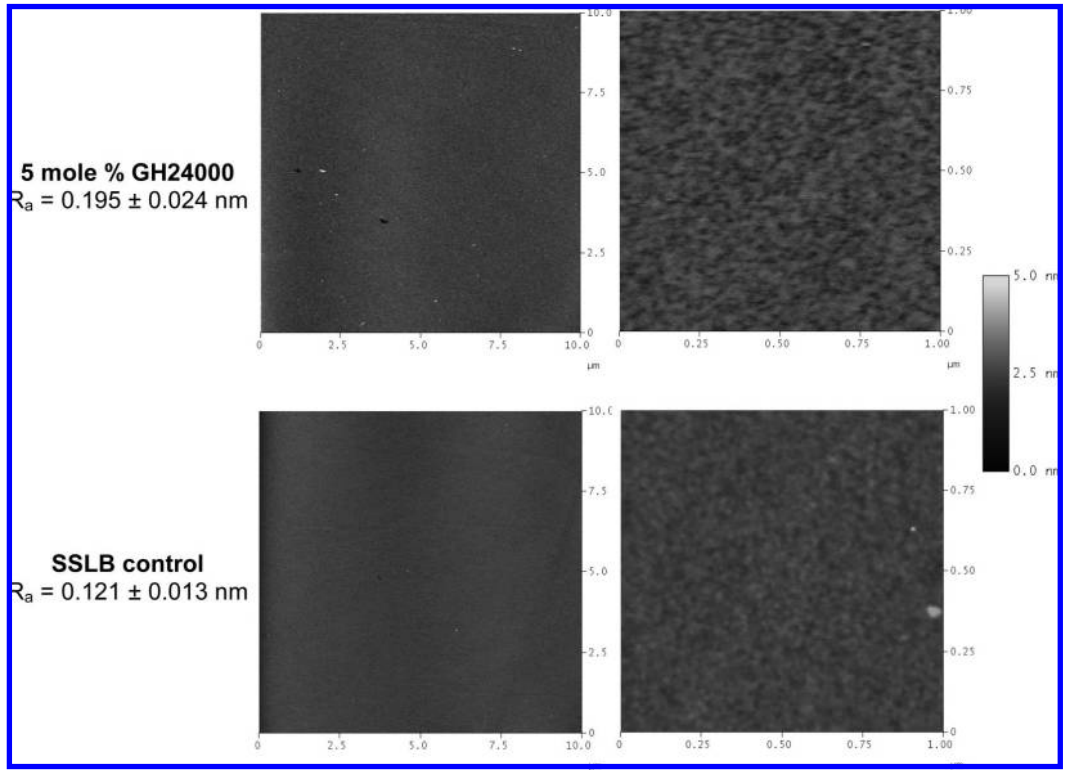

Figure 9. AFM images of bilayers imaged in standard buffer (10 mM Tris, 100 mM NaCl adjusted to pH 8 using NaOH). The bilayer formed on the 5 mol % GH24000-tethered system is shown in the top images. For comparison, an SSLB control formed directly on a SiO_x substrate is shown in the bottom images. For both samples, a 10 × 10 μm scan is shown on the left and a 1 × 1 μm scan is shown on the right. The mean roughness, R_a, is also indicated.

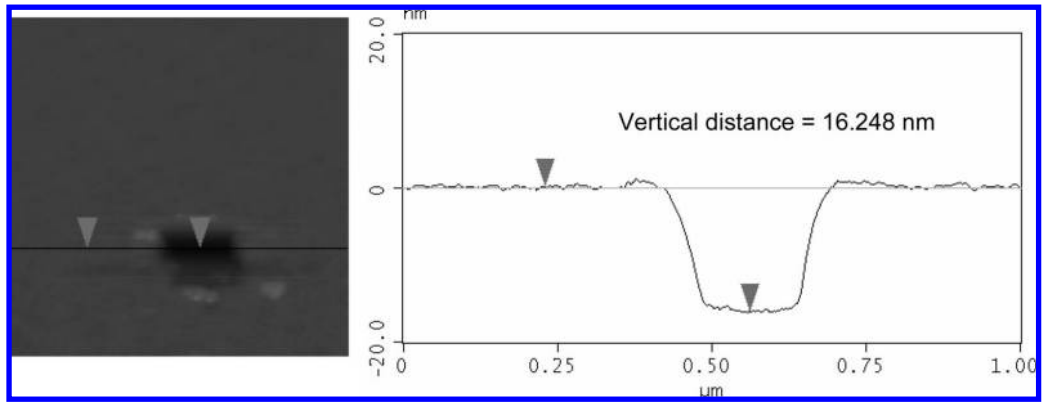

Figure 10. Thickness of a 5 mol % GH24000-tethered bilayer measured by AFM in which the tethered bilayer was removed by high-force contact mode AFM.

Table 2. Scaling Parameters for GH24000

number of monomers	103
number of monomers per Kuhn segment	7 (from polystyrene)
number of Kuhn segments, N	15
Kuhn segment length, a	18 Å (from polystyrene)
Flory radius, R_F	91 Å

PEG Kuhn segment values of $N = 77/3 = 25.7$ and $a = 11$ Å, we predict the mushroom-to-brush transition to emerge at 1.2 mol % lipopolymer for their system. Though this is not in exact agreement with the observed isotherms, it is much closer than predicted using monomeric values. Naumann et al.[31] also studied the polymer brush behavior of grafted PEG-based lipopolymers. They used monomeric PEG values to calculate a brush extension length of 43.8 Å for a 45 repeat unit PEG, which was significantly less than experimentally observed thicknesses (between 65 and 80 Å). They concluded that the PEG was in a conformation that was even more extended than predicted. Using Kuhn segment values, the predicted brush extension is actually 98.4 Å, more than twice the thickness calculated using monomeric PEG values.

Although the fundamental need for an increased separation distance is a major driving force behind the development of polymer-tethered lipid bilayers, very few groups have directly investigated the separation distance that is created by the polymer tethers.[32] Using AFM, we measured the separation distance for a 5 mol % GH24000 to be 11.2 nm for a region removed by contact mode AFM scratching. Using the de Gennes scaling theory for polymers anchored to an interface, the extension length

(31) Naumann, C. A.; Brooks, C. F.; Fuller, G. G.; Knoll, W.; Frank, C. W. *Langmuir* **1999**, *15*, 7752–7761.

(32) Kiessling, V.; Tamm, L. K. *Biophys. J.* **2003**, *84*, 408–418.

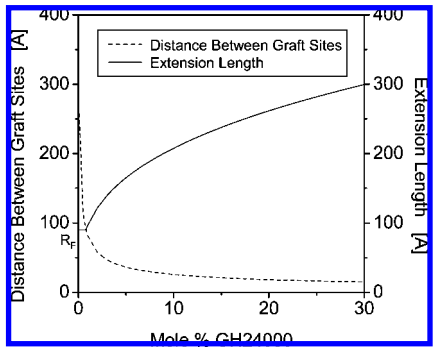

Figure 11. Theoretical polymer conformational behavior based on the de Gennes scaling theory.[30] The mushroom-to-brush transition is predicted to occur at 0.8 mol % GH24000.

(i.e., separation distance between the substrate and bilayer) was predicted to be 16.5 nm for a 5 mol % GH24000 tether (see Figure 11). The value obtained for the separation distance by AFM is relatively close to the predicted value and confirms that this polymer-tethered bilayer system is able to create separation distances significantly greater than the 1−2 nm separation distances measured for solid-supported lipid bilayers. This also indicates that the de Gennes scaling theory can be a useful tool for predicting and tailoring separation distances for these polymer-tethered bilayers according to the specific application requirements.

It is important to remember that polystyrene Kuhn values were used to estimate the scaling parameters for our glycoacrylate polymer. In the future, actual Kuhn values should be determined to obtain more accurate predictions. Nevertheless, this separation distance found for our 5 mol % GH24000-tethered bilayer is significantly larger than that reported for a similar PEG-based tethered bilayer developed by Kiessling and Tamm.[32] For a 3 mol % PEG-tethered bilayer, fluorescence interference-contrast microscopy (FLIC) was used to measure a separation distance of 3.9 nm, which they reported to be close to the value predicted by the de Gennes scaling theory (4.8 nm). However, incorrect parameters of monomer units and monomer lengths were used instead of Kuhn segment values to calculate the extension length as discussed previously. When Kuhn segment values are used ($N = 25.7$ and $a = 11$ Å), the extension length is actually predicted to be 10.5 nm, nearly 3 times greater than what was measured.

Homogeneity. Although bilayer homogeneity may not be critical for all applications, our goal was to develop a homogeneous model membrane system for maximum flexibility of use. Several reports on polymer-tethered lipid bilayers have highlighted a variety of heterogeneities visible by fluorescence microscopy.[24,27,33] These heterogeneities are likely due to different process-specific features, and this discussion will focus primarily on model membranes formed using LB transfer of the polymer-tethered monolayer that serves as the proximal bilayer leaflet. LB transfer is a dynamic process that can substantially alter the properties of the transferred monolayer and must be optimized to achieve the desired monolayer state. For a given monolayer at a specific transfer pressure, the transfer speed can critically affect the monolayer quality. Therefore, preliminary studies were conducted to investigate the effect of transfer speed for each monolayer composition at various transfer pressures (data not shown). These studies were used to find optimal LB transfer conditions that produce the most homogeneous monolayer with transfer ratios approaching ideal. At 25 mN/m, relatively homogeneous monolayers were obtained with transfer ratios approaching ideal using a transfer speed of 10.0 mm/min for all mixed monolayer compositions used in these studies. It should be noted that we were unable to form homogeneous bilayers on monolayers transferred at nonoptimal transfer speeds that resulted in poor monolayer quality (data not shown). These bilayers displayed stripe inhomogeneities that disappeared when the transfer speed was optimized, which was similar to results reported by Purrucker et al. for a poly(2-methyl-2-oxazoline)-tethered membrane.[27]

Bilayer homogeneity and continuity can be very important for applications such as separation devices. Although fluorescence microscopy is a relatively straightforward technique for studying fluorescently labeled bilayers, the resolution is typically on the order of several hundred nanometers. Defects or holes smaller than this, which can lead to device failure, can go undetected via fluorescence microscopy. Using AFM, which has a lateral resolution on the order of 2−10 nm, we found comparable lateral homogeneity in a 5 mol % GH24000-tethered bilayer and solid-supported bilayer control. However, both samples had several hole defects that were between 100 and 300 nm wide (below the resolution of our fluorescence microscopy objective). The source of these defects is not known. They may have been due to chemical contamination on the substrate surface or particulate contamination during preparation and imaging. The substrates were cleaned extensively, and care was taken to keep the samples clean. However, the sample preparation and imaging were not done in a clean room. They could also have been due to slight local variations in the lipid interactions which alter healing and spreading capabilities. If this is the case, various types of annealing (for example, mechanical or temperature cycling) during the monolayer formation at the air−water interface could be used to minimize the presence of these defects. For applications in which bilayer continuity and integrity are essential for proper function, electrochemical experiments examining the effect of these defects on bilayer "leakiness" could be performed. The vertical distance of these defects is ∼2 nm (less than half of the thickness of the bilayer), and they may simply be defects in the top leaflet that do not critically affect the electrochemical integrity of the system. However, complete AFM studies need to be done for the other percentage of GH24000 bilayers to ensure that lateral homogeneity can be achieved for all mixtures.

Lateral Mobility. When the diffusion of a lipid probe in a polymer-tethered lipid bilayer is considered, there are two main differences between this system and a solid-supported lipid bilayer: (1) The presence of swollen polymer tethers significantly changes the viscosity of the aqueous environment adjacent to the proximal leaflet relative to the thin 1−2 nm water layer neighboring a solid-supported bilayer proximal leaflet. (2) Tethered lipid groups that do not have the same lateral freedom as the free lipids (egg-PC) are present in the proximal leaflet.

Literature studies examining the viscosity of the adjacent fluid have shown that the viscosities of polymer tethers and cushions (i.e., no covalent attachment between the polymer and bilayer) are several orders of magnitude higher than the viscosity of bulk water.[24,34] Kühner et al. determined that the viscosity of their polyacrylamide gel used to cushion a lipid bilayer was ∼0.5 P.[34] Wagner and Tamm reported a viscosity of ∼9 P for their PEG-based polymer tether system.[24] These are both significantly higher than the viscosity of bulk water (0.008 P), which is taken as an approximation for the viscosity of the water layer adjacent to the solid-supported lipid bilayer. However, Kühner et al. reported that this increased viscosity did not affect lipid mobility within the proximal leaflet. They found that the "apparent frictional

(33) Munro, J. C.; Frank, C. W. *Langmuir* **2004**, *20*, 10567–10575.

(34) Kühner, M.; Tampé, R.; Sackmann, E. *Biophys. J.* **1994**, *67*, 217–226.

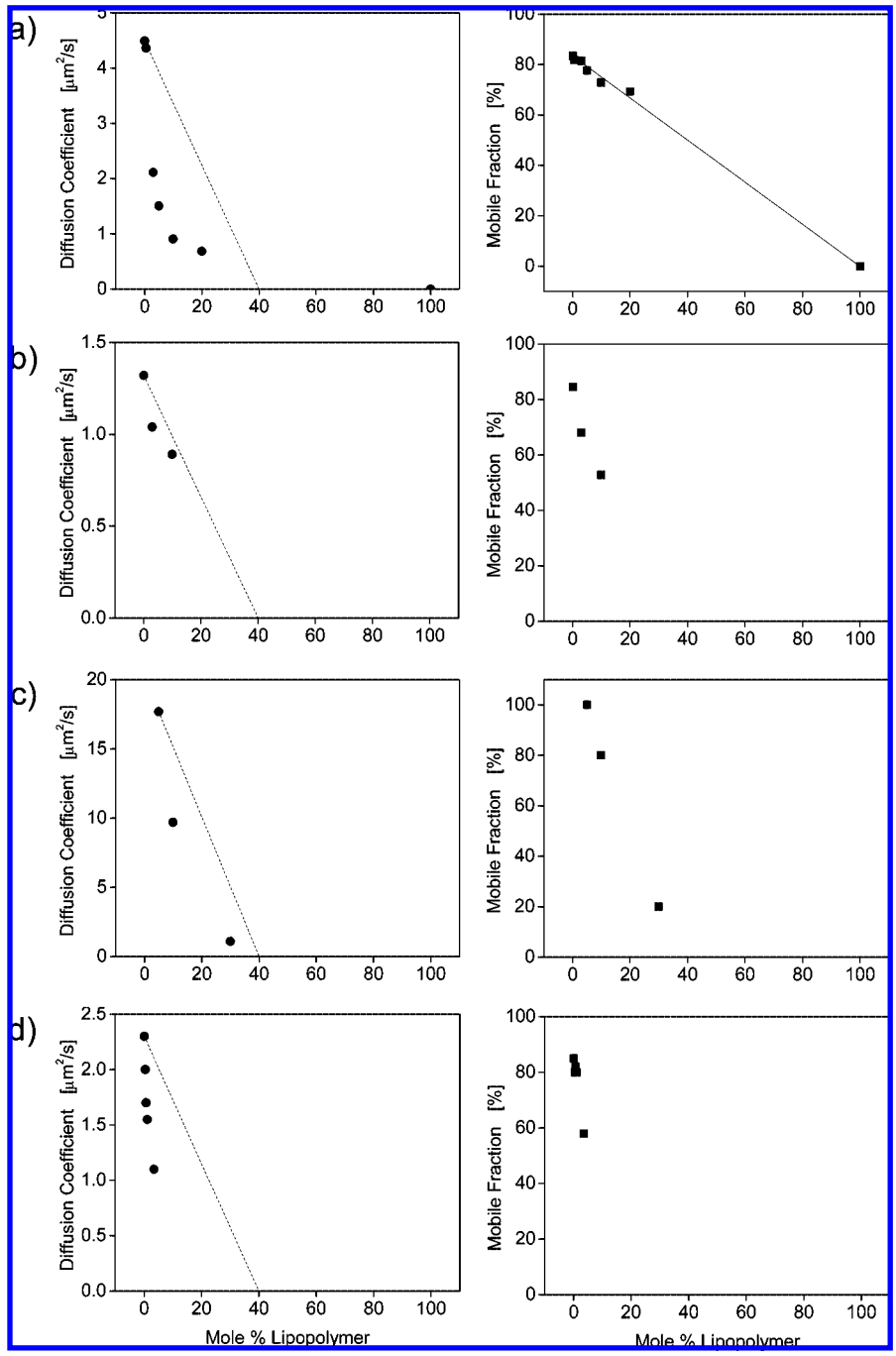

Figure 12. Distal leaflet lateral mobility data for various polymer-tethered lipid bilayers. The dotted lines in the diffusion coefficient data represent the theoretical prediction for obstructed diffusion with a percolation threshold at ~40% immobile particles. Data are (a) shown for our GH24000 lipopolymer and (b−d) taken from literature reports on a (b) PEG-based lipopolymer,[24] (c) poly(ethyloxazoline)-based lipopolymer,[25] and (d) PEG-based lipopolymer[33] formed via self-assembly (note that (d) shows data for lipid probes incorporated in both leaflets).

coefficient" and diffusion coefficient of the proximal leaflet lipid probes were the same with or without the polyacrylamide gel cushion adjacent to the proximal leaflet. They also found that polymer viscosity effects were only significant when membrane components that extended beyond the membrane into the polymer cushion were observed.[34] Deverall et al. confirmed this using a polymer-tethered lipid bilayer as a model system for studying obstructed diffusion.[26] This system was well described using a free-area model of diffusion, which implied that the polymer tethers did not interact with neighboring lipids to impede their diffusion. These data indicate that the polymer viscosity does not significantly affect the lipid diffusion and is not the main source for the trends in the diffusion coefficient and mobile fraction observed in our studies. Therefore, we can also conclude that the conformation of the polymer tethers, which will directly impact the viscosity of the adjacent fluid, will not have a substantial influence on the fluidity of the lipids in the bilayer, but rather will become more important in controlling and tailoring the separation distance. However, viscosity effects will still need to be considered when membrane components that extend beyond the boundaries of the bilayer are incorporated.

The second major aspect of lipid mobility in polymer-tethered lipid bilayers to consider is the presence of tethered lipids in the proximal leaflet. These do not have the same lateral freedom as the surrounding free lipids since the polymers are covalently attached to the substrate. Deverall et al. found that even lipid

groups attached to polymers that are not covalently bound to the substrate behave as immobile obstacles on the time scales of typical experiments.[26] They validated this treatment of the tethered lipids as immobile obstacles by data fits to theoretical models for obstructed diffusion assuming hard-core repulsion that give a percolation threshold at ~40% immobile particles.[35−37]

The description of tethered lipids as immobile obstacles accounts for the mobility data reported for proximal leaflet probes, but it does not explain the data trends observed for lipid probes in the distal leaflet. As shown in Figure 12a, the distal leaflet diffusion coefficients measured for our GH24000-tethered bilayers deviate negatively from the theoretical predictions for obstructed diffusion by immobile obstacles discussed above in which a percolation threshold is reached at ~40% tethering. This negative deviation is also seen with other reported polymer-tethered lipid bilayer systems, as shown in Figure 12b−d. Also, the mobile fraction data do not follow behavior described by a percolation threshold in which a constant mobile fraction should be seen prior to the threshold, followed by a sudden decrease. Instead, a continuous decrease in mobile fraction with increasing percentage of tethering is observed. These trends imply that the lateral motion of the lipid probes is impaired beyond what is experienced in the proximal leaflet.

One possible cause for this is that the immobile tethered lipids in the proximal leaflet strongly couple to lipids in the distal leaflet and hinder the mobility of those lipids. Merkel et al. found that the friction coefficient between a fluid leaflet and an immobile leaflet was significantly greater than between two fluid leaflets, implying a strong coupling effect between bilayer leaflets.[38] Therefore, it is possible that there are actually two populations of lipid probes present in the distal leaflet: (1) immobilized lipid probes (on the time scale of the experiments) via coupling to immobile proximal leaflet lipids and (2) mobile lipid probes that are obstructed by the immobile lipid probes.

If only the second population of lipid probes were present in the distal leaflet, the same data trends as in the free-area percolating model would be observed. However, the existence of this first population of immobile lipid probes would lead to negative deviation in the diffusion coefficient behavior from the free-area percolating model. It would also result in a linear decrease in mobile fraction with increasing percentage of tethered lipids since the fraction of immobile probes would increase directly proportional to the fraction of tethered lipids as seen in Figure 12a. It should be noted that the mobile fractions shown in Figure 12b−d do not follow this same decrease and actually indicate lower mobile fractions than would be expected using this hypothesis. This effect may be related to the large heterogeneities seen in several of the final bilayers.[24,33] Although this proposed model is plausible, it should be remembered that FRAP experiments average the behavior of many probes. Therefore, any explanation must be confirmed by additional techniques such as single-particle tracking.[39]

Conclusions

In these studies, we have specifically investigated the separation distance and lateral fluidity of homogeneous bilayer assemblies. We can now take these data in combination with the understanding of the monolayer at the air−water interface and knowledge of how to control the LB transfer of the monolayer onto a substrate to understand, predict, and create tailorable polymer-tethered bilayer macromolecular assemblies in a controlled fashion. In these studies, we used a single lipopolymer sample ($M_w = 24\,000$) as a representative system for investigation and found how the lateral fluidity and separation distance changed with the tethering density. These results could be extended to various molecular weight polymers in a straightforward fashion. It was demonstrated that the de Gennes scaling theory could be used to reliably predict polymer conformations and separation distances simply on the basis of Kuhn segment knowledge. In addition, we found that lateral fluidity was a function of the tethering density (i.e., immobilized proximal leaflet lipids) rather than the polymer conformation (i.e., viscosity). Using this knowledge, one could tailor a final bilayer to have an independently specified separation distance and lateral fluidity. However, it should be noted that the polymer conformation is not an insignificant parameter of these tethered bilayer assemblies. Although stability studies were not conducted, Albertorio et al.[40] found that the polymer conformation in tethered bilayers was directly related to the stability of the bilayer in air. They showed that bilayers formed on PEG tethers in a brush conformation yielded high air stability and did not show signs of damage or stress after removal from an aqueous environment, whereas bilayers on PEG tethers in the mushroom conformation showed significant damage.

Further work needs to be conducted to confirm that laterally homogeneous bilayers with predictable separation distances can be formed using all mixed monolayer compositions. However, these studies demonstrate that we have developed a viable biomimetic system that is well-defined and whose final bilayer properties can be reliably tailored.

Acknowledgment. We acknowledge financial support provided by the NSF-MRSEC Program through the Center on Polymer Interfaces and Macromolecular Assemblies (Grant NSF-DMR 9808677) and the NASA HEDS Program (Grant NAG8-1843).

LA8022997

(35) Saxton, M. J. *Biophys. J.* **1987**, *52*, 989–997.
(36) Almeida, P. F. F.; Vaz, W. L. C.; Thompson, T. E. *Biochemistry* **1992**, *31*, 7198–7210.
(37) Saxton, M. J. *Biophys. J.* **1993**, *64*, 1053–1062.
(38) Merkel, R.; Sackmann, E.; Evans, E. *J. Phys. (Paris)* **1989**, *50*, 1535–1555.
(39) Saxton, M. J.; Jacobson, K. *Annu. Rev. Biophys. Biomol. Struct.* **1997**, *26*, 373–399.
(40) Albertorio, F.; Diaz, A. J.; Yang, T. L.; Chapa, V. A.; Kataoka, S.; Castellana, E. T.; Cremer, P. S. *Langmuir* **2005**, *21*, 7476–7482.